

Analysis and Rate Optimization of GFDM-based Cognitive Radios

A. Mohammadian, M. Baghani, C. Tellambura, *Fellow, IEEE*

Abstract—Generalized frequency division multiplexing (GFDM) is suitable for cognitive radio (CR) networks due to its low out-of-band (OOB) emission and high spectral efficiency. In this paper, we thus consider the use of GFDM to allow an unlicensed secondary user (SU) to access a spectrum hole. However, in an extremely congested spectrum scenario, both active incumbent primary users (PUs) on the left and right channels of the spectrum hole will experience OOB interference. While constraining this interference, we thus investigate the problem of power allocation to the SU transmit subcarriers in order to maximize the overall data rate where the SU receiver is employing Matched filter (MF) and zero-forcing (ZF) structures. The power allocation problem is thus solved as a classic convex optimization problem. Finally, total transmission rate of GFDM is compared with that of orthogonal frequency division multiplexing (OFDM). For instance, when right and left interference temperature should be below 10 dBm, the capacity gain of GFDM over OFDM is 400%.

Index Terms—CR network, GFDM, Signal-to-interference-plus-noise ratio, Adjacent channel interference, Rate optimization problem

I. INTRODUCTION

THE development of fifth generation (5G) wireless networks faces the challenge of congested and limited wireless spectral resources [1]. The main reasons for that are the massive growth of wireless data traffic and the assignment of almost all spectrum bands below 6-GHz bands to existing wireless and cellular applications. However, primarily due to usage patterns, many spectrum bands temporarily become spectrum holes. A spectrum hole is a free frequency band in a certain location in which the licensed (primary) users are not transmitting temporarily. Such spectrum holes can be accessed by unlicensed users or secondary users (SUs) under the interweave cognitive radio (CR) paradigm.

In 5G, the physical layer (PHY) maybe based on orthogonal frequency division multiplexing (OFDM) or Generalized frequency division multiplexing (GFDM) [2]. Although OFDM is robust against frequency selective fading, its high out-of-band (OOB) interference may render it unsuitable for CR networks [3]-[6]. GFDM has thus been proposed [7], [8]. GFDM uses multiple symbols per subcarrier and shapes each subcarrier by a circularly-shifted prototype filter. The spectral efficiency of GFDM is higher than that of OFDM because the former uses only single cyclic prefix (CP) for an entire block. As well, GFDM can reduce the latency of PHY layer [9], the main requirement of Tactile Internet [10]. In addition, due to the shaping of each subcarrier individually, the OOB emission of GFDM is low [11] and can be further reduced by better design of filtering [12]. Multicarrier signaling methods

are especially vulnerable against the carrier frequency offset (CFOs) between transmitter and receiver, which arise due to Doppler effects, thermal effects, aging and others. In OFDM, a CFO kills the perfect orthogonality among all the subcarriers, resulting in the lowering of the signal to interference ratio (SIR). In contrast, in GFDM, a receiver filter can improve robustness against CFOs [13], which maximizes the SIR. Thus, these advantages ensure that GFDM is an attractive modulation method for 5G and CR networks [14], [15]. However, GFDM incurs additional implementation complexity which has been improved in [16]–[19]. Due to these advantages, especially the low OOB emissions, we consider the use of GFDM for unlicensed CR users in this paper.

Unlicensed SUs may access the primary user (PU) spectrum in two different modes. First, in underlay mode, they access simultaneously with active PU transmissions, but ensure that the resulting interference on PU nodes is less than a specified interference threshold. Thus, in this mode, dynamic interference management is the key – which can be achieved by several techniques such as secondary transmit power control, guard regions and/or proactive interference cancellation. Unfortunately, these techniques will constrain the achievable SU rates. Moreover, the burden of implementing such techniques falls on the secondary network. Second, in the interweave mode, the SUs access spectrum holes only [20]. And that is the scenario investigated in this paper. The challenge, however, is the accurate and dynamic sensing of spectrum holes. Two common sensing methods are energy detection and cyclostationary detection. [21] reveals GFDM has a better complementary receiver operating characteristic (ROC) compared to OFDM based on energy detection method. In addition, Reference [22] shows signal detection improves with GFDM due to its cyclostationary autocorrelation properties compared to OFDM. In light of these advantages, GFDM appears as a suitable candidate for interweave CR networks.

Although optimal power allocation improves the SU network performance, the interference on incumbent PUs network must be below guaranteed interference thresholds. Specifically, in this paper, we consider the problem of the OOB emission of SU over spectrum hole affecting the active PUs in the adjacent channels. The resource allocation for OFDM CR is first considered in [23], and other heuristic and fast resource allocation methods are proposed in [24], [25]. However, GFDM uses non-orthogonality of subcarriers whereas OFDM uses orthogonal ones. Thus the power allocation problem is completely different between GFDM and OFDM. Thus, the signal-to-interference-plus-noise ratio (SINR) is more complicated. In [26], GFDM power allocation in underlay cognitive radio is

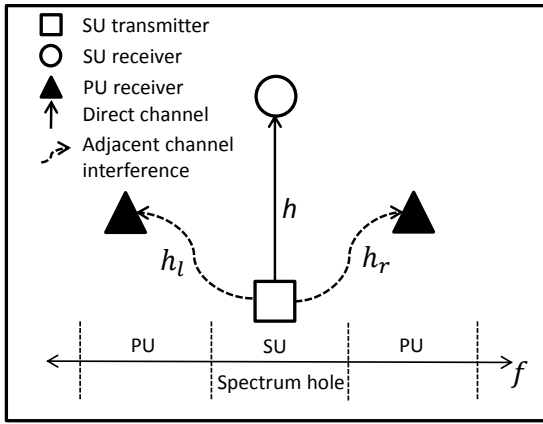


Fig. 1: The cognitive radio model.

solved via genetic algorithms. In [27], CR resource allocation is done by particle swarm optimization (PSO). However, although the optimization problem is not convex due to the interference on subcarriers, the dual Lagrange multiplier method is used as analytical solution in [27]. Also, the metaheuristic approaches for non-convex optimization problems, e.g. PSO, do not guarantee to reach to the global optimum due to the lack of any theoretical basis. To the best of our knowledge, no analytical resource allocation strategies to increase the spectral efficiency of GFDM SUs for different receiver structures have been published before.

In Fig. 1, we consider an SU link consisting of an SU transmitter and SU receiver operating over a spectrum hole in which PUs are not present temporarily. Also, two PUs are active in left and right channels of the spectrum hole. Furthermore, the interference levels from PUs to the SU link are assumed to be negligible. We consider GFDM system for different cases: 1) uniform and non-uniform power allocation to subcarriers, 2) different number of subsymbols and 3) two common MF and ZF receivers. Moreover, a frequency selective slow fading channel is considered. We assume that channel state information (CSI) of all the links (e.g., SU transmitter to receiver and SU transmitter to PU receivers) is available at the SU transmitter. It can estimate the CSI of SU-SU links by using any classic channel training, estimation, and feedback mechanisms. It can estimate the CSI of SU-PU links by utilizing beacon signals transmitted by PUs and by exploiting channel reciprocity. In this paper, we investigate the problem of maximizing the SU rate under the constraints of maximum tolerable interference power on PU bands and maximum transmit power. This problem is solved for the aforementioned scenarios, and GFDM is compared with OFDM to determine the relative advantages of GFDM for CR networks.

In detail, the contributions of this paper are follows.

- For the SU link, we consider two different standard receiver techniques; namely matched filter (MF) and zero forcing (ZF). We derive their SINR and SIR as function of subcarrier power allocations. Moreover, the accuracy of the derived formulas are verified by simulations.
- Adjacent channel interference (ACI) of the SU on the

active users on right and left channels of the utilized spectrum hole are derived and incorporated to define the constraints of rate optimization problem. For this purpose we derive the power spectral density (PSD) of GFDM non-equal subcarrier power allocations.

- The maximization problems for the total rate of SU with GFDM in a CR network are defined. After convexifying the optimization problems by adding an interference threshold, an analytical solution to the optimal subcarrier power allocations is proposed by utilizing the Lagrange method.
- The impact of the number of subsymbols, a critical parameter in GFDM, on the symbol error rate (SER) performance and OOB emission of MF and ZF receivers is investigated, and their sum rate performances are considered.
- Finally, we compare the spectral efficiencies of GFDM and OFDM. For different power allocations, we show that GFDM achieves higher efficiency than OFDM due to its lower OOB emission. Note that the proposed algorithm provides high SU transmission rate while satisfying the tolerable interference temperature constraints on PU spectrum. These advantages are suitable for opportunistic spectrum access in practical applications, e.g. CR TV white space (TVWS) transmission.

The rest of this paper is organized as follows: the system model is presented in Section II. The SINR and signal-to-noise ratio (SNR) of received symbols in MF and ZF receivers and their SER are derived in Section III. We derive the power spectral density (PSD) of GFDM signal for non-identical power scaling for subcarriers and obtain the ACI on the right and left channels in Section IV. The rate optimization problems are defined and solved in Section V. Simulation and numerical results in Section VI verify the accuracy of the analytical expressions and confirm the benefits of the optimization results. Finally, concluding remarks are provided in Section VII.

II. SYSTEM MODEL

In our system model (Fig. 1), the SU uses GFDM and the SU transmitter-receiver channel is denoted by h . We assume the PUs are active in the two adjacent channels of the spectrum hole which is used by the SU. The gains of these two channels are denoted by h_r and h_l . These gains will determine the amount of ACI falls on the PUs.

In GFDM, let $\vec{s} = [s(0), \dots, s(MK - 1)]^T$ be $MK \times 1$ complex data vector with independent and identically distributed (i.i.d) entries, which are chosen from 2^μ - QAM complex constellation where μ is the modulation order. GFDM contains K subcarriers which transmit data of M time-slots. The input data vector is assigned to M time-slots according to $\vec{s} = \left[[s_0]^T, [s_1]^T, [s_2]^T, \dots, [s_{M-1}]^T \right]^T$ where $[s_m] = [s_{m,0}, s_{m,1}, s_{m,2}, \dots, s_{m,K-1}]^T$. Thus, $s_{m,k}$ is the transmitted data symbol in k -th subcarrier of m -th time-slot.

The GFDM signal per frame may be written as

$$x[n] = \sum_{k=0}^{K-1} \sum_{m=0}^{M-1} \sqrt{\alpha_k} s_{m,k} g_{Tx_m}[n] e^{j2\pi \frac{(k-K-1)}{K^2} n} \quad (1)$$

where α_k is power allocated to the k -th subcarrier, $g_{Tx_m}[n] = g_{Tx}[n - mK]_{MK}$ is circularly shifted version of the transmitted prototype filter $g_{Tx}[n]$ and $0 \leq n \leq MK-1$. Furthermore, by representing output samples of GFDM modulator as a $MK \times 1$ vector $\vec{x} = [x[0], x[1], x[2], \dots, x[MK-1]]^T$, one block of GFDM signal is given by $\vec{x} = \mathbf{A}\vec{s}$, where \mathbf{A} is a $MK \times MK$ modulation matrix given by $[\mathbf{A}]_{n,mM+k} = g_{Tx_m}[n] e^{j2\pi n \frac{(k-K-1)}{K^2}}$.

The signal $x[n]$ is sent over the wireless channel. Given sufficiently long CP, perfect synchronization and knowledge of the channel impulse response, the receiver can remove the CP. As a result, circular convolution with channel impulse response can be considered as $\vec{y} = \vec{h} \otimes \vec{x} + \vec{w}$, where \otimes denotes circular convolution and w is additive white Gaussian noise (AWGN). Then, frequency domain equalization (FDE) is used and The equalized signal is $\vec{u} = \vec{x} + \vec{w}_{eq}$, where $\vec{w}_{eq} = \text{IFFT} \left\{ \frac{\vec{W}}{\vec{H}} \right\}$, \vec{W} and \vec{H} are the noise vector and the channel response in frequency domain, respectively. The resulted vector goes through GFDM demodulator and vector of the estimated symbols is calculated by $\vec{s} = \mathbf{B}\vec{u}$, where \mathbf{B} is receiver matrix.

The receiver matrix for MF and ZF linear GFDM receivers are equal to \mathbf{A}^H and \mathbf{A}^{-1} , respectively. In the MF receiver \mathbf{B} is selected to maximizing the signal-to-noise ratio (SNR) for each symbol without considering interference. In GFDM, however, subcarriers and subsymbols are not mutually orthogonal. Thus, the inter-subcarrier interference will limit the performance of the MF receiver. To eliminate it, the linear ZF receiver can be used. However, the ZF receiver has the drawback of enhancing the additive noise.

With either of these receivers, each estimated symbol at a given subcarrier and time-slot can be written as [17]

$$\hat{s}_{m',k'} = r_{m',k'} + w_{eq,m',k'} \quad (2)$$

where $w_{eq,m',k'}$ is the equivalent noise and $r_{m',k'}$ is equal to

$$r_{m',k'} = \frac{1}{\sqrt{\alpha_{k'}}} \sum_{n=0}^{MK-1} x[n] g_{Rx_m'}^* e^{-j2\pi \frac{(k'-K-1)}{K^2} n} \quad (3)$$

where $g_{Rx}[n]$ is the receive filter impulse response, $g_{Rx_m}[n] = g_{Rx}[n - mK]_{MK}$ is circularly shifted version of that and $(\cdot)^*$ denotes the conjugate operator.

III. RECEIVED SINR DERIVATIONS

In this section, we derived the SINR for the MF and ZF receivers.

A. MF receiver

As mentioned before, the MF receiver suffers from self-generated interference. Nevertheless, SNR per subcarrier in

this receiver is maximized without considering this interference. By using (1), (2), (3) and substituting $m = m'$ and $k = k'$, the output of this receiver (2) can be rewritten as

$$\hat{s}_{m',k'} = s_{m',k'} + n_{m',k'} + w_{eq,m',k'}^{MF} \quad (4)$$

where $n_{m',k'} = r_{m',k'} - s_{m',k'}$ is interference noise. To derive SINR, the variance of each term is needed. First, variance of interference noise is derived as (see Appendix A).

$$\sigma_{n_{m',k'}}^2 = \mathbb{E}[n_{m',k'} n_{m',k'}^*] = \frac{1}{\alpha_{k'}} \sum_{k=0}^{K-1} \alpha_k f_{m',k'}(k) - \bar{p}_s \quad (5)$$

where $\mathbb{E}[\cdot]$ is the ensemble average operator and

$$f_{m',k'}(k) = \sum_{m=0}^{M-1} \sum_{n_1=0}^{MK-1} \sum_{n_2=0}^{MK-1} \alpha_k \bar{p}_s g_{Rx_m}[n_1] \times g_{Rx_m}^*[n_2] g_{Rx_m'}^*[n_1] g_{Rx_m'}[n_2] e^{j2\pi \frac{(k-k')}{K} (n_1 - n_2)} \quad (6)$$

Second, the variance of equivalent noise is calculated as [8]

$$\sigma_{w_{eq,m',k'}^{MF}}^2 = \frac{N_0}{MK \alpha_{k'}} \sum_{p=0}^{MK-1} \left| \frac{G_{m',k'}^{MF}[-p]}{H[p]} \right|^2 \quad (7)$$

where $G_{m',k'}^{MF}[p]$ is frequency response of $g_{Rx-MF}^*[n] e^{-j2\pi \frac{(k'-K-1)}{K^2} n}$, $H[p]$ is channel frequency response and N_0 is noise power density. Due to (5) and (7), the SINR experienced by SU receiver for MF at k -th subcarrier and m -th time-slot after the frequency selective AWGN channel can be expressed as

$$\Gamma_{m',k'}^{MF} = R_T \frac{\bar{p}_s}{\sigma_{n_{m',k'}}^2 + \sigma_{w_{eq,m',k'}^{MF}}^2} = R_T \frac{\bar{p}_s \alpha_{k'}}{\sum_{k=0}^{K-1} \alpha_k f_{m',k'}(k) - \bar{p}_s \alpha_{k'} + C_{m',k'}^{MF}} \quad (8)$$

where $C_{m',k'}^{MF} = \alpha_{k'} \sigma_{w_{eq,m',k'}^{MF}}^2$, $R_T = \frac{MK}{MK + N_{CP}}$ and $\bar{p}_s = \mathbb{E}\{s_{m',k'} s_{m',k'}^*\}$ is average power of data symbols which for $2^\mu - \text{QAM}$ modulation is equal to $\bar{p}_s = \frac{2(2^\mu - 1)}{3}$. Furthermore, SER can be calculated for a GFDM system over frequency selective channel with MF receiver by summation of probability of symbols decoded being in error for $2^\mu - \text{QAM}$ as [8]

$$P_s^{MF} = 2 \left(\frac{\mu - 1}{\mu MK} \right) \sum_{m=0}^{M-1} \sum_{k=0}^{K-1} \text{erfc} \left(\sqrt{\frac{3\Gamma_{m',k'}^{MF}}{2(2^\mu - 1)}} \right) - \frac{1}{MK} \left(\frac{\mu - 1}{\mu} \right)^2 \sum_{m=0}^{M-1} \sum_{k=0}^{K-1} \text{erfc}^2 \left(\sqrt{\frac{3\Gamma_{m',k'}^{MF}}{2(2^\mu - 1)}} \right) \quad (9)$$

where $\text{erfc}(x)$ is the complementary error function. The SER is an important parameter of quality of service (QoS) and (9) provides the means to test the accuracy of (8).

B. ZF receiver

Unlike MF, ZF eliminates self-generated interference, but enhances additive noise. By considering (2), ZF estimated data of m -th time-slot in k -th subcarrier can be derived as

$$\hat{s}_{m',k'} = s_{m',k'} + w_{eq,m',k'}^{ZF}. \quad (10)$$

Due to (7), the received SNR at k -th subcarrier and m -th time-slot given the frequency selective and AWGN channel may be expressed as

$$\Gamma_{m',k'}^{ZF} = R_T \frac{\bar{P}_s}{\sigma_{w_{eq,m',k'}^{ZF}}^2} = R_T \frac{\bar{P}_s \alpha_{k'}}{C_{m',k'}^{ZF}}. \quad (11)$$

Moreover, SER of GFDM with ZF receiver may be given by [8]

$$P_s^{ZF} = 2 \left(\frac{\mu-1}{\mu MK} \right) \sum_{m=0}^{M-1} \sum_{k=0}^{K-1} \operatorname{erfc} \left(\sqrt{\frac{3\Gamma_{m',k'}^{ZF}}{2(2^\mu-1)}} \right) - \frac{1}{MK} \left(\frac{\mu-1}{\mu} \right)^2 \sum_{m=0}^{M-1} \sum_{k=0}^{K-1} \operatorname{erfc}^2 \left(\sqrt{\frac{3\Gamma_{m',k'}^{ZF}}{2(2^\mu-1)}} \right). \quad (12)$$

Note that variance of equivalent noise is derived based on receiver filter which is different for MF and ZF.

IV. ADJACENT CHANNEL INTERFERENCE

In our model, the PUs are active in right and left adjacent channels of the spectrum hole. Thus, they will experience destructive interference because of the OOB emissions of the SU. To study this effect, we assume frequency selective slow fading channels for PUs. However, with a sufficient cyclic prefix, the frequency selective channel is equivalent to multiple flat fading channels in frequency domain. For small frequency bin, the channel frequency response is constant across each frequency bin which are denoted by $H_r(d)$ and $H_l(d)$ for right and left neighboring channel responses in each frequency bin, respectively, an example is shown in Fig. 2 for four subcarriers. The total ACI is calculated through summation of ACI on each frequency bin which is derived by multiplying the adjacent channel power (ACP) in each frequency bin by channel gains. Therefore, total ACI at right neighboring channel may be expressed as

$$P_{ACI} = \sum_{d=K+1}^{2K} P_{AC}(f_d) H_r(d-K) \quad (13)$$

where $P_{AC}(f_d)$ is ACP in frequency interval $[f_d - 1/(2T_s), f_d + 1/(2T_s)]$ where $f_d = \frac{K+2d+1}{2T_s}$ is center of each frequency interval, T_s is one time-slot duration and d is the index of frequency bin. To find ACP in each frequency bin, the PSD of signal is derived as (see Appendix B)

$$S_{xx}(f) = \frac{\bar{P}_s}{MT_s} \sum_{k=0}^{K-1} \alpha_k S_{GG}(f - \frac{(k - \frac{K-1}{2})}{T_s}) \quad (14)$$

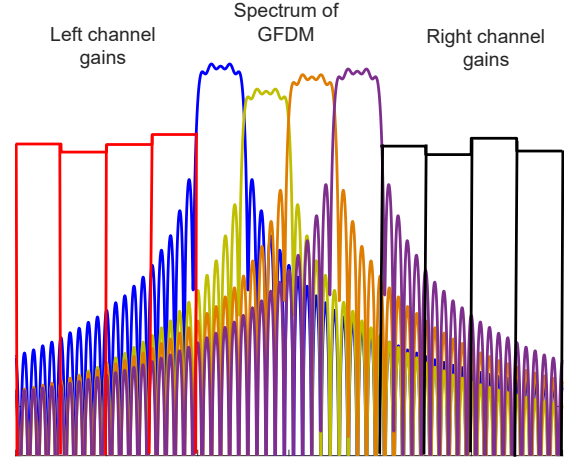


Fig. 2: PSD of GFDM and left and right channel gains for four subcarriers.

where $S_{GG}(f) = \sum_{m=0}^{M-1} |G_{Tx_m}(f)|^2$ and $G_{Tx_m}(f)$ is frequency response of each filter. According to (13) and (14), ACI in right adjacent channel can be derived as

$$P_r = \sum_{k=0}^{K-1} \alpha_k T_r(k) \quad (15)$$

where

$$T_r(k) = \frac{\bar{P}_s}{MT_s} \sum_{d=K+1}^{2K} H_r(d-K) \int_{f_d-1/(2T_s)}^{f_d+1/(2T_s)} S_{GG}(f - \frac{(k - \frac{K-1}{2})}{T_s}) df. \quad (16)$$

Similarly, ACI in left adjacent channel is calculated by

$$P_l = \sum_{k=0}^{K-1} \alpha_k T_l(k) \quad (17)$$

where

$$T_l(k) = \frac{\bar{P}_s}{MT_s} \sum_{d=K+1}^{2K} H_l(d-K) \int_{-f_d-1/(2T_s)}^{-f_d+1/(2T_s)} S_{GG}(f - \frac{(k - \frac{K-1}{2})}{T_s}) df. \quad (18)$$

These two derived powers must be below the acceptable interference thresholds of the left and right PU channels. This constraint will be incorporated into the rate optimization problem subsequently.

V. PROBLEM FORMULATION

We next formulate and solve the maximization of the total transmission rate of the SU under interference constraint for both MF and ZF receivers. Technically, we aim to find the optimal set of power allocations $(\alpha_0, \alpha_1, \dots, \alpha_{K-1})$.

$$\alpha_k = \left[\frac{M}{\left[\sum_{k'=0}^{K-1} \sum_{m'=0}^{M-1} \gamma_{m'+Mk'} (f_{m',k'}(k) - \bar{p}_s) \right] + \gamma_{MK} + \gamma_{MK+1} T_r(k) + \gamma_{MK+2} T_l(k)} - \frac{Q_n + C_{0,k}^{MF}}{\bar{p}_s} \right]^+ \quad (25)$$

A. MF receiver

With the MF receiver, according to (8),(15) and (17), the rate optimization problem can be formulated as

$$\max_{\alpha_k} \sum_{0 \leq k \leq K-1} \sum_{k'=0}^{K-1} \sum_{m'=0}^{M-1} \log(1 + \Gamma_{m',k'}^{MF}) \quad (19)$$

$$s.t. \quad \sum_{k=0}^{K-1} \alpha_k < \alpha_{\max} \quad (20)$$

$$\sum_{k=0}^{K-1} \alpha_k T_r(k) < Q_r \quad (21)$$

$$\sum_{k=0}^{K-1} \alpha_k T_l(k) < Q_l \quad (22)$$

where Q_r and Q_l are the interference temperature limits for the right and left adjacent channels, respectively. Furthermore, α_{\max} is the maximum total power that is divided between K subcarriers. However, because $\Gamma_{m',k'}^{MF}$ is a rational expression of α_k 's, the objective function (19) is not convex. To overcome the non-convexity of objective function, we introduce an additional constraint to original problem [28] which is given by

$$\sum_{k=0}^{K-1} \alpha_k f_{m',k'}(k) - \bar{p}_s \alpha_{k'} < Q_n \quad \forall m', k'. \quad (23)$$

As shown in (4), due to self-generated interference in MF receiver, extracted symbols contain interference noise with which the total power of these terms have been calculated in (5). Thus, inequality constraint (23) can be interpreted as the sum of self-generated interference in each time-slot of each subcarrier being less than the self-interference noise threshold Q_n . By setting this threshold Q_n appropriately, we can improve the system performance. The resulting convex optimization problem is solved by utilizing the method of Lagrange multipliers to encapsulate all the constraints:

$$\begin{aligned} L(\alpha, \gamma) &= \sum_{k'=0}^{K-1} \sum_{m'=0}^{M-1} \log\left(1 + \frac{\bar{p}_s \alpha_{k'}}{Q_n + C_{m',k'}^{MF}}\right) \\ &+ \sum_{k'=0}^{K-1} \sum_{m'=0}^{M-1} \gamma_{m'+Mk'} \left(Q_n - \sum_{k=0}^{K-1} \alpha_k f_{m',k'}(k) + \bar{p}_s \alpha_{k'}\right) \\ &+ \gamma_{MK} (\alpha_{\max} - \sum_{k=0}^{K-1} \alpha_k) + \gamma_{MK+1} \left(Q_r - \sum_{k=0}^{K-1} \alpha_k T_r(k)\right) \\ &+ \gamma_{MK+2} \left(Q_l - \sum_{k=0}^{K-1} \alpha_k T_l(k)\right) \end{aligned} \quad (24)$$

where γ_j , $j = 0, \dots, MK + 2$, are Lagrange multipliers. Due to the standard convex form of this problem, the Karush-Kuhn-Tucker (KKT) conditions, which are the first order necessary and sufficient conditions for optimality, yield the optimal solution. Thus, the optimal power allocated to each subcarrier as a function of the Lagrange multipliers is obtained as (25), where $[x]^+ = \max(0, x)$ and k is the subcarrier index. From the Lagrangian duality, (24) should be minimized on Lagrangian multipliers. Thus, they can updated by using the sub-gradient method. The subgradient update equations are given by

$$\begin{aligned} \gamma_{m'+Mk'}(t+1) &= \left[\gamma_{m'+Mk'}(t) + \zeta \left(\sum_{k=0}^{K-1} \alpha_k f_{m',k'}(k) - \bar{p}_s - Q_n \right) \right]^+ \\ \gamma_{MK}(t+1) &= \left[\gamma_{MK}(t) + \zeta \left(\sum_{k=0}^{K-1} \alpha_k - \alpha_{\max} \right) \right]^+ \\ \gamma_{MK+1}(t+1) &= \left[\gamma_{MK+1}(t) + \zeta \left(\sum_{k=0}^{K-1} \alpha_k T_r(k) - Q_r \right) \right]^+ \\ \gamma_{MK+2}(t+1) &= \left[\gamma_{MK+2}(t) + \zeta \left(\sum_{k=0}^{K-1} \alpha_k T_l(k) - Q_l \right) \right]^+ \end{aligned} \quad (26)$$

where ζ denotes the positive step size. Thus, the entire iterative process for solving this rate optimization problem is given in Algorithm. 1. Due to the convexity of our problem, the duality gap is zero and the proposed algorithm is optimal. We should note that if equal power for subcarriers are considered, we can set $\alpha_k = \alpha$. Thus, the optimum amount of the power which satisfies all constraints could be derived as

$$\alpha_{opt} = \min \left\{ \frac{Q_n}{\sum_{k=0}^{K-1} f_{m',k'}(k) - \bar{p}_s}, \frac{\alpha_{\max}}{K}, \frac{Q_r}{\sum_{k=0}^{K-1} T_r(k)}, \frac{Q_l}{\sum_{k=0}^{K-1} T_l(k)} \right\}. \quad (27)$$

This solution is the just the power level that will not violate all the constraints.

B. ZF receiver

Like the MF receiver, the ZF rate maximization problem is formulated as

$$\begin{aligned} \max_{\alpha_k} \sum_{0 \leq k \leq K-1} \sum_{k'=0}^{K-1} \sum_{m'=0}^{M-1} \log(1 + \Gamma_{m',k'}^{ZF}) \quad (28) \\ s.t. \quad (20), (21), (22). \end{aligned}$$

Algorithm 1 Rate optimization

- 1: Initialize the maximum number of iteration I_{\max} and convergence condition ε_γ
 - 2: set $t \leftarrow 1$
 - 3: **do while** $\sum_{i=1}^{K-1} |\alpha_k(t) - \alpha_k(t-1)| > \varepsilon_\gamma$ and $t < I_{\max}$
 - 4: $t \leftarrow t + 1$
 - 5: Obtain α_k by using derived formula
 - 6: Update the Lagrange multipliers
 - 7: **end do**
 - 8: **return**
-

Since this problem is convex, the Lagrangian for this optimization problem is obtained as

$$\begin{aligned}
 L(\alpha, \gamma) &= \sum_{k'=0}^{K-1} \sum_{m'=0}^{M-1} \log\left(1 + \frac{\overline{p_s} \alpha_{k'}}{C_{m',k'}^{ZF}}\right) \\
 &+ \gamma'_0 (\alpha_{\max} - \sum_{k=0}^{K-1} \alpha_k) + \gamma'_1 (Q_r - \sum_{k=0}^{K-1} \alpha_k T_r(k)) \\
 &+ \gamma'_2 (Q_l - \sum_{k=0}^{K-1} \alpha_k T_l(k))
 \end{aligned} \quad (29)$$

where γ'_i , $i = 0, 1, 2$, are Lagrangian multipliers. Based on KKT conditions, the optimal power allocated to each subcarrier is calculated as

$$\alpha_k = \left[\frac{M}{\gamma'_0 + \gamma'_1 T_r(k) + \gamma'_2 T_l(k)} - \frac{C_{0,k}^{ZF}}{\overline{p_s}} \right]^+. \quad (30)$$

The subgradient equations for updating the lagrangian coefficients in each iteration can be derived as

$$\begin{aligned}
 \gamma'_0(t+1) &= \left[\gamma'_0(t) + \zeta \left(\sum_{k=0}^{K-1} \alpha_k - \alpha_{\max} \right) \right]^+ \\
 \gamma'_1(t+1) &= \left[\gamma'_1(t) + \zeta \left(\sum_{k=0}^{K-1} \alpha_k T_r(k) - Q_r \right) \right]^+ \\
 \gamma'_2(t+1) &= \left[\gamma'_2(t) + \zeta \left(\sum_{k=0}^{K-1} \alpha_k T_l(k) - Q_l \right) \right]^+.
 \end{aligned} \quad (31)$$

As before, the optimization problem (28) is solved with Algorithm 1. Same as previous section, the optimum problem for uniform power allocation is derived as

$$\alpha_{opt} = \min \left\{ \frac{\alpha_{\max}}{K}, \frac{Q_r}{\sum_{k=0}^{K-1} T_r(k)}, \frac{Q_l}{\sum_{k=0}^{K-1} T_l(k)} \right\}. \quad (32)$$

Note that all the derived analytical formulas are general and hold for arbitrary signaling alphabet, numbers of subcarriers and subsymbols and any type of prototype filter. Indeed, in all cases, our proposed algorithms for MF and ZF can provide optimal power allocation to maximize the rate of SU.

TABLE I: GFDM, channel and system parameters

parameter	Value
Mapping	16 – QAM
Filter type	Raised – cosine
Roll-off factor	0.15
Symbol duration (T_s)	33.3 μ s
Number of subcarriers (K)	64
Number of sub symbols (M)	5,15
Subcarrier spacing ($\frac{1}{T_s}$)	30 KHz
Signal Bandwidth ($\frac{K}{T_s}$)	1.92 MHz
CP length (N_{cp})	10
Channel length (N_{ch})	10
Variance of each tap	$(10^{\frac{-i}{N_{ch}-1}})_{i=0, \dots, N_{ch}-1}$
Number of OFDM subcarriers	64

VI. SIMULATION AND NUMERICAL RESULTS

In this section, the derived SERs and PSD are validated with simulations and optimization results are presented. The parameters of GFDM and channel are shown in Table I. The Averaged periodogram algorithm with 50% overlap and Hanning window is used to estimate the PSD and length of FFT (fast Fourier transform) is set to 65536. Monte carlo simulation uses 1000 GFDM symbols per run. Moreover, the value of threshold is equal to 0.0001 and $\alpha_{max} = 55$ dBm. In Section VI-A, the SER of (9) and (12) are verified by simulations. The accuracy of derived PSD for GFDM modulated signal (14) is validated by simulation. In Section VI-B, the performance of proposed Algorithm 1 for both GFDM and OFDM with uniform and non-uniform power allocation to subcarriers is evaluated.

A. Verification of derived results

In Fig. 3, the SER of GFDM with MF or ZF receivers are compared with that of OFDM. E_s is average transmit power which for GFDM is equal to $E_s = \frac{\overline{p_s}}{K} \sum_{k=0}^{K-1} \alpha_k$ and N_0 is normalized to one. On the one hand, as can be seen, the simulation results verify the analytical derivation of SER for MF and ZF receivers in (9) and (12), respectively. Therefore, we can conclude that the derived formulas for SINR of MF (8) and SNR of ZF (11) are accurate. Also, with GFDM, ZF outperform MF, which has performance approximately near that of OFDM. On the other hand, more subsymbols degrade the SER performance of both MF and ZF receivers. This degradation is due to noise enhancement in both receivers when the number of subsymbols is increased. Note that α_{max} has been chosen according to Fig. 3.

Fig. 4 shows the PSD of GFDM with different numbers of subsymbols is compared with that of OFDM. A set of random power allocations for subcarriers is generated and has been utilized for all three scenarios. As can be seen, the simulation results verify the derived PSD (14). Moreover, the increased number of subsymbols decreases the PSD rapidly on adjacent channels. Indeed, OOB emission decreases by increasing the number of GFDM subsymbols. This result is in contrast with effect of increasing number of subsymbols on SER performance. Thus, although more subsymbols decreases

TABLE II: Optimum values of Q_n extracted for different interference power constraints by considering two different number of subsymbols .

Subsymbols	-20 dBm	-15 dBm	-10 dBm	-5 dBm	0 dBm	5 dBm	10 dBm	15 dBm	20 dBm	25 dBm
$M = 5$	0.0022	0.0044	0.0155	0.03	0.07	0.15	0.34	0.7	1.435	1.435
$M = 15$	0.0133	0.0233	0.04	0.091	0.1933	0.47	1.02	2.11	2.11	2.11

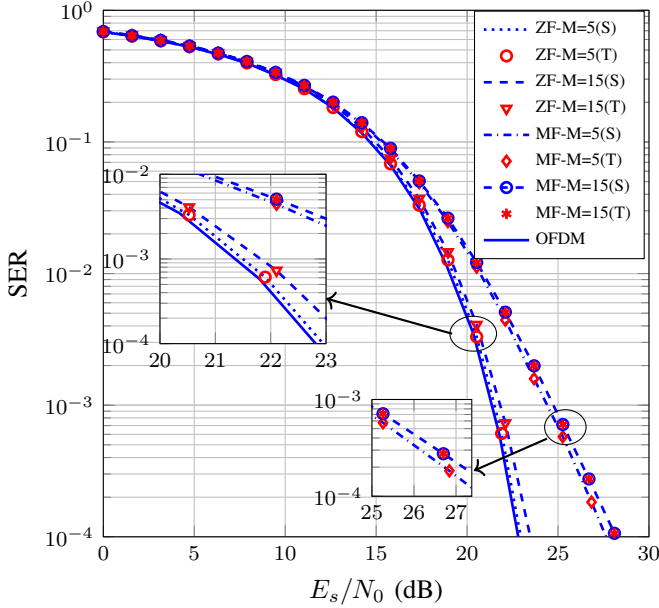


Fig. 3: SER of GFDM (with MF and ZF receivers) and of OFDM. Legend: S=simulation and T=theory.

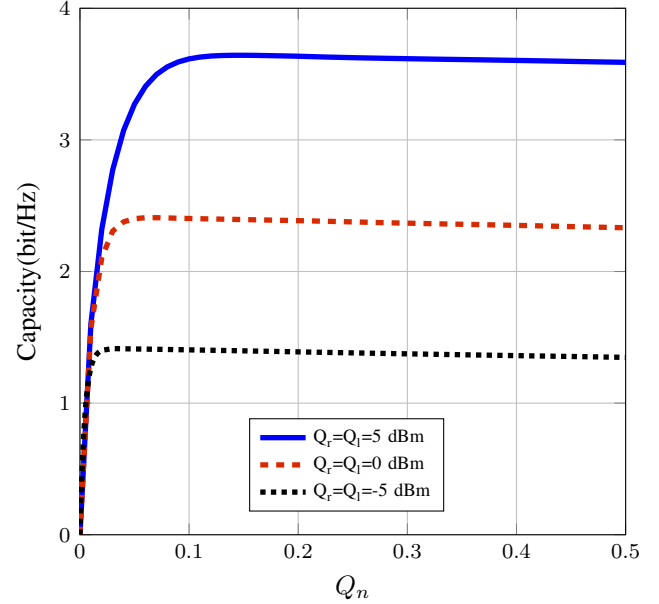


Fig. 5: Capacity of the GFDM with MF receiver versus Q_n for three constant interference power constraints.

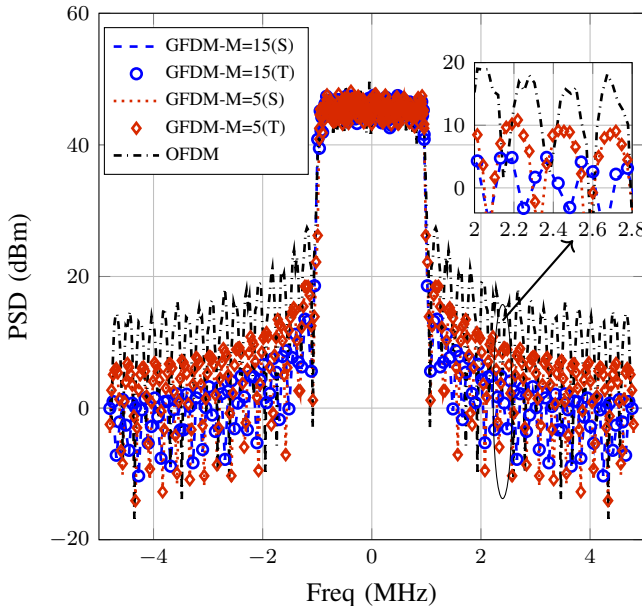


Fig. 4: PSDs of GFDM and OFDM signals.

the OOB emission, the SER also degrades. The SER is affected due to in-band noise which influences the transmission rate while OOB emission indicates the out-of-band noise which plays a main role in the CR constraints. In the next section, we investigate the trade-off between these two effects of

increasing the number of subsymbols.

B. Optimization Results

In this part, we evaluate the performance of GFDM and OFDM systems subject to the CR constraints. As the first step, we investigate the effect of the self-interference threshold Q_n on the transmission rate to find the best value of Q_n . Since this value helps us to convert the optimization problem into convex form, determining the right value so important. After that, the rate optimization problem is solved by using the Lagrangian method. Finally, the simulation results are presented and the performance of the proposed algorithm is compared between GFDM system with ZF and MF receivers and OFDM system and the influence of number of subsymbols is considered as well.

As mentioned, the amount of self-interference, considered as an extra constraint and transformed the problem into convex optimization problem, has an impact on the transmission rate of the SU. To evaluate this effect and find the optimal value, we solve the optimization problem for the fixed value of interference power constraint. We sweep Q_n over a range to find the optimum one which maximizes the total transmission rate. Fig. 5 shows the transmission rate versus value of Q_n for three amounts Q_r and Q_i (5 dBm, 0 dBm and -5 dBm) where the number of subcarriers and subsymbols are set to 64 and 5, respectively. As expected, this power allocation problem

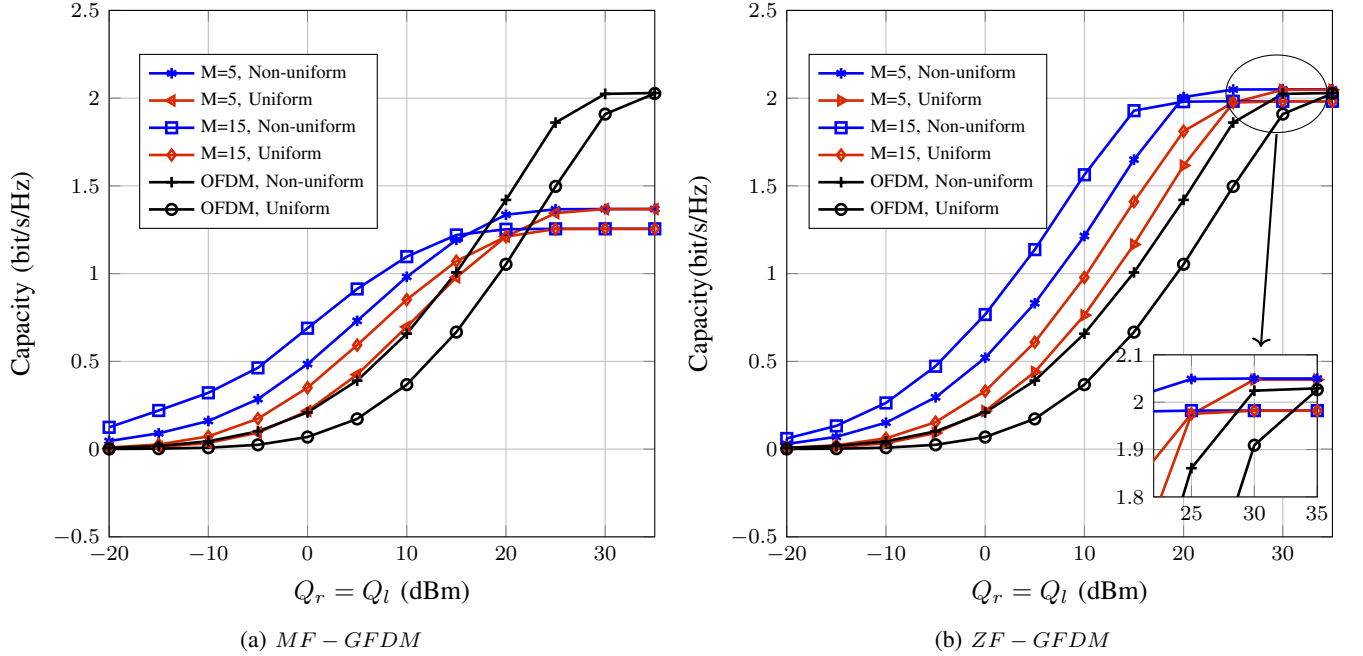


Fig. 6: Total sum rate of the SU of GFDM with MF and ZF receivers in compare with OFDM.

has an optimum value. By utilizing the same procedure, for two number of subsymbols ($M = 5$ and $M = 15$) with different values of interference power constraint, the optimization problem is solved and the optimum values of Q_n are given in Table II. In the following, these fixed value of Q_n is chosen for the rate optimization problem.

Fig. 6 represents the results of the rate optimization problems for GFDM and OFDM systems. The achievable transmission rate for GFDM system with MF and ZF receivers are shown in Fig. 6a and Fig. 6b, respectively, in which the results contain uniform and non-uniform power allocations to subcarriers. As expected, in both cases of MF and ZF, non-uniform power allocation has better performance in compare with allocating equal power to all subcarriers. On the one hand, in Fig. 6a, when the interference power constraint is not dominant and the OOB emission does not cause any problem in CR e.g. $Q_r = Q_l = 30$ dBm, due to the non orthogonality of GFDM and self-interference, OFDM system should achieves higher rate. Similarly, although, the SER performance of ZF receiver is lower than OFDM, the transmission rate of that is higher than OFDM due to the inserting one CP to each GFDM frame including symbol of M time-slots. Now when the amount of interference power constraints decrease and become dominant, where is sufficient for the CR system, the GFDM system in both case of MF and ZF receivers achieves higher rates which is caused by lower OOB radiation of GFDM system in compare with OFDM system. On the other hand, we investigate the impact of number of subsymbols for GFDM system with both MF and ZF receivers. we can conclude that in low amount of interference power constraint, GFDM system with both type of receivers transmits higher rate in case of $M = 15$ than $M = 5$ due to the lower OOB emission and is declared in Fig. 4. But, since the SER performance of GFDM system is decreased by increasing the

number subsymbols, when the interference power constraint is not dominant, the achievable rate in case of $M = 5$ is higher than $M = 15$. Consequently, in the CR system, the GFDM system with MF and ZF receivers transmits higher rate in compare with OFDM system in both case of uniform and non-uniform power allocation to subcarriers. Also, increasing the number of subsymbols can help us to achieve higher rate.

To compare the performance of ZF and MF receivers, the total transmitted rates of GFDM system for $M = 5$ subsymbols are illustrated in Fig. 7. When the interference power constraint is not dominant, because the SER performance ZF receiver is better than that of MF receiver, the former achieves higher transmission rate. But, when the interference power constraint decreases, the rate of MF receiver exceeds that of the ZF receiver. This phenomena is caused by the decreasing amount of interference appearing in SINR (8) when the amount of powers allocated to subcarriers decrease. Since MF receiver maximizes the SNR without considering the interference, when the interference can be neglected, the MF receiver has the best performance. Consequently, when the interference power constraint is non-dominant, the system with ZF receiver achieves a higher rate. But, by decreasing the interference power constraint and eliminating the interference, the system with MF receiver achieves higher transmission rate than the one with ZF receiver.

Fig. 8 shows the total optimized transmit power versus the interference power constraint. GFDM with ZF and MF receivers achieves higher transmit power than that with OFDM. The reason is that the interference power constraint becomes dominant in GFDM later than in OFDM, which is due to lower OOB emission of GFDM system. On the other hand, more subsymbols leads to decrease OOB emission. Thus, in case of $M = 15$, higher power is transmitted in compare with $M = 5$. All of these results confirm the previous results

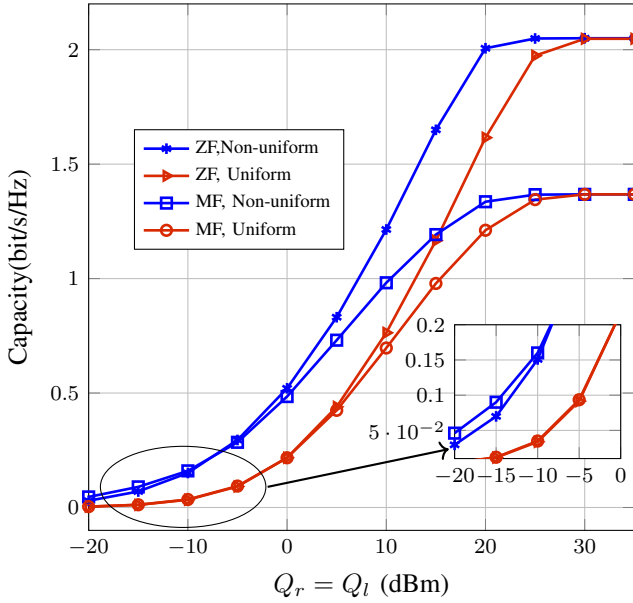


Fig. 7: Total sum rate of GFDM with ZF and MF receivers for $M = 5$.

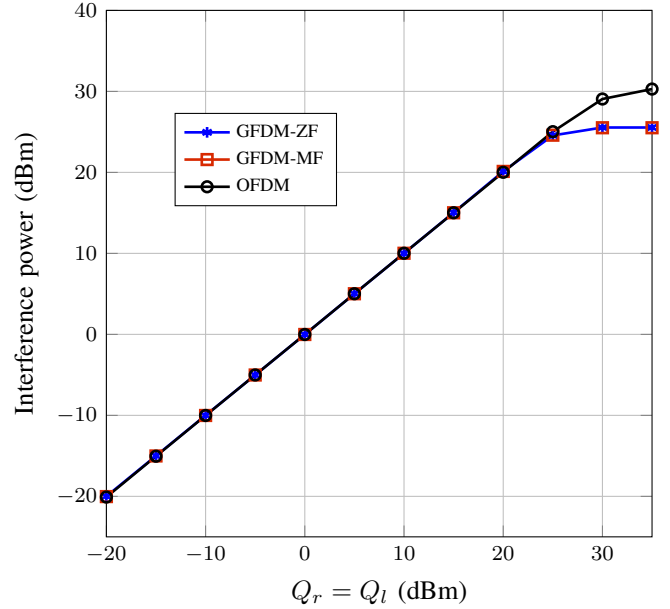


Fig. 9: Interference power versus different values of Q_r .

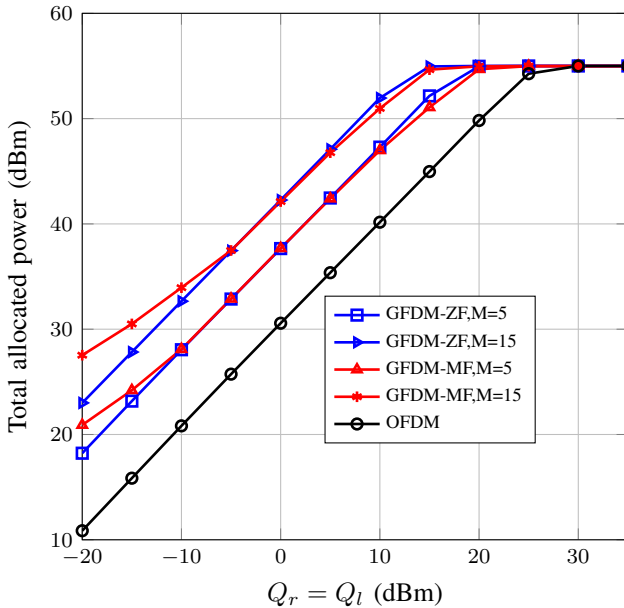


Fig. 8: Total transmitted power versus different power interference constraints.

in which utilizing the GFDM system with higher number of subsymbols in lower interference power constraint can satisfy the CR system demand. Moreover, when the interference power constraint decreases, higher transmit power is achieved by the system with the MF receiver in comparison with ZF receiver. This observation also agrees with Fig. 7.

Fig. 9 represents the average interference power based on power allocation results versus interference power which contains the GFDM and OFDM systems. Both MF and ZF receivers are considered for GFDM system. As expected, the average interference power is approaching to specific value

of interference power constraint. This figure shows that the optimization realizes the interference level and not exceed the allowed value which is determined for interference power constraint.

VII. CONCLUSION

This paper evaluated the performance of a GFDM based CR network where unlicensed secondary users access the primary spectrum. Specifically, we considered a secondary user transmitting on a spectrum hole whose left and right adjacent bands are occupied by primary users. To constrain the ACI on the left and right channels, we derived the PSD of GFDM signal with the non-equal power subcarriers. To determine the sum rate of the SU, we derived the SINR and SNR for MF and ZF receivers, respectively. The SER and GSD expressions were validated over by simulations over frequency selective fading and AWGN channels. The simulation results also showed that the SER performance degrades and OOB leakage decreases when the number of subsymbols increases.

We also optimized the SU rate subject the ACI constraints on left and right channels and maximum total power. In MF case, by adding the new constraint on limitation of self-generated interference the problem was converted to convex form. Also, the maximum self-generated interference limit of this constraint which maximizes the sum rate of the SU was extracted by simulation. The resulting rate optimization problems were solved by using the Lagrangian method. We compared the total transmitted rate of the SU, utilizing GFDM with MF and ZF receivers, with OFDM for both uniform and non-uniform power allocations to subcarriers.

The simulations show that the total rate of SU for our proposed power allocation algorithm is significantly higher than uniform power allocation in all cases and that GFDM achieves higher data throughput than OFDM in a CR network where the ACI constraints are dominant. In this case, MF receiver

can achieve more total rate compared with ZF receiver. But when the ACI constraints are not dominant, the ZF receiver achieves better SER and data rates in comparison with MF. In this case, OFDM performs roughly equal to ZF and better than MF. Consequently, GFDM based CR nodes with MF and ZF receivers achieve high data rates, which can be enhanced by increasing the number of subsymbols. In future works, other impairments which affect the OOB emission of SU on spectrum of PUs like as RF impairments specially nonlinear power amplifier can be investigated.

APPENDIX A

Due to (3) and (4), variance of interference noise can be written by

$$\begin{aligned}\sigma_{n_{m',k'}}^2 &= \mathbb{E}[(r_{m',k'} - s_{m',k'})(r_{m',k'}^* - s_{m',k'}^*)] \\ &= \mathbb{E}[r_{m',k'} r_{m',k'}^*] + \mathbb{E}[s_{m',k'} s_{m',k'}^*] \\ &\quad - 2\text{real}(\mathbb{E}[r_{m',k'} s_{m',k'}^*])\end{aligned}\quad (33)$$

By considering normalized prototype pulse shape ($\sum_{n=0}^{MK-1} |g_{Tx}[n]|^2 = 1$), each part of (33) can be calculated as

$$\begin{aligned}\mathbb{E}[r_{m',k'} r_{m',k'}^*] &= \frac{1}{\alpha_{k'}} \sum_{k=0}^{K-1} \alpha_k f_{m',k'}(k) \\ \mathbb{E}[s_{m',k'} s_{m',k'}^*] &= \bar{p}_s \\ \mathbb{E}[r_{m',k'} s_{m',k'}^*] &= \bar{p}_s \sum_{n=0}^{MK-1} |g_{m'}[n]|^2 = \bar{p}_s\end{aligned}\quad (34)$$

According to (33) and (34), (5) is derived.

APPENDIX B

According to (1), the continuous form of GFDM signal by concatenating frames is expressed as

$$x(t) = \sum_{v=-\infty}^{\infty} \sum_{k=0}^{K-1} \sum_{m=0}^{M-1} \sqrt{\alpha_k} s_{m,k,v} g_{Tx_m}(t - vT_B) e^{j2\pi \frac{(k-\frac{K-1}{2})}{T_s} t}\quad (35)$$

Where $g_{Tx_m}(t)$ is continuous form of $g_{Tx_m}[n]$ with the length of MT_s and T_B is block duration which is equal to MT_s . To calculate its PSD, autocorrelation of $x(t)$ is derived as

$$\begin{aligned}R_{xx}(t, \tau) &= \bar{p}_s \sum_{v=-\infty}^{\infty} \sum_{k=0}^{K-1} \sum_{m=0}^{M-1} \alpha_k g_{Tx_m}(t - vT_B) \\ &\quad g_{Tx_m}^*(t - \tau - vT_B) e^{j2\pi \frac{(k-\frac{K-1}{2})}{T_s} \tau}\end{aligned}\quad (36)$$

Since GFDM yields cyclostationary process, $R_{xx}(t, \tau) = R_{xx}(t + MT_s, \tau)$, the average of $R_{xx}(t, \tau)$ over one period is calculated as

$$\begin{aligned}\bar{R}_{xx}(\tau) &= \frac{1}{MT_s} \int_0^{MT_s} R_{xx}(t, \tau) dt \\ &= \frac{\bar{p}_s}{MT_s} \left(\sum_{m=0}^{M-1} g_m(\tau) \otimes g_m(-\tau) \right) \sum_{k=0}^{K-1} \alpha_k e^{j2\pi \frac{(k-\frac{K-1}{2})}{T_s} \tau}\end{aligned}\quad (37)$$

By taking the Fourier transform of (37), (14) is derived.

REFERENCES

- [1] J. Andrews, S. Buzzi, W. Choi, S. Hanly, A. Lozano, A. Soong, and J. Zhang, "What will 5G be?," *IEEE J. Sel. Areas Commun.*, vol. 32, no. 6, pp. 1065–1082, June 2014.
- [2] G. Wunder, P. Jung, M. Kasparick, T. Wild, F. Schaich, Y. Chen, S. T. Brink, I. Gaspar, N. Michailow, A. Festag, L. Mendes, N. Cassiau, D. Ktenas, M. Dryjanski, S. Pietrzyk, B. Eged, P. Vago, and F. Wiedmann, "5G NOW: Non-orthogonal, asynchronous waveforms for future mobile applications," *IEEE Commun. Mag.*, vol. 52, no. 2, pp. 97–105, Feb. 2014.
- [3] S. Haykin, "Cognitive radio: brain-empowered wireless communications," *IEEE J. Sel. Areas Commun.*, vol. 23, no. 2, pp. 201–220, Feb. 2005.
- [4] Y. C. Liang, K. C. Chen, G. Y. Li, and P. Mahonen, "Cognitive radio networking and communications: an overview," *IEEE Trans. Veh. Technol.*, vol. 60, no. 7, pp. 3386–3407, Sept. 2011.
- [5] M. Mirahmadi, A. Al-Dweik, and A. Shami, "BER reduction of OFDM based broadband communication systems over multipath channels with impulsive noise," *IEEE Trans. Commun.*, vol. 61, no. 11, pp. 4602–4615, Nov. 2013.
- [6] J. Van De Beek and F. Berggren, "Out-of-band power suppression in OFDM," *IEEE Commun. Lett.*, vol. 12, no. 9, pp. 609–611, Sept. 2008.
- [7] G. Fettweis, M. Krondorf, and S. Bittner, "GFDM - generalized frequency division multiplexing," in *Proc. IEEE Veh. Technol. Conf. (VTC Spring)*, Apr. 2009, pp. 1–4.
- [8] N. Michailow, M. Matthäi, I. S. Gaspar, A. N. Caldeilla, L. L. Mendes, A. Festag, and G. Fettweis, "Generalized frequency division multiplexing for 5th generation cellular networks," *IEEE Trans. Commun.*, vol. 62, no. 9, pp. 3045–3061, Sept. 2014.
- [9] I. Gaspar, L. Mendes, M. Matthäi, N. Michailow, A. Festag, and G. Fettweis, "LTE-compatible 5G PHY based on generalized frequency division multiplexing," in *Proc. ISWCS*, Aug. 2014, pp. 209–213.
- [10] G. P. Fettweis, "The tactile internet: Applications and challenges," *IEEE Veh. Technol. Mag.*, vol. 9, no. 1, pp. 64–70, March 2014.
- [11] M. Matthäi, N. Michailow, I. Gaspar, and G. Fettweis, "Influence of pulse shaping on bit error rate performance and out of band radiation of generalized frequency division multiplexing," in *Proc. IEEE ICC Workshop*, June 2014, pp. 43–48.
- [12] S. Han, Y. Sung, and Y. H. Lee, "Filter design for generalized frequency-division multiplexing," *IEEE Trans. Signal Process.*, vol. 65, no. 7, pp. 1644–1659, April 2017.
- [13] B. Lim and Y. C. Ko, "SIR analysis of OFDM and GFDM waveforms with timing offset, CFO and phase noise," *IEEE Trans. Wireless Commun.*, vol. PP, no. 99, pp. 1–1, 2017.
- [14] M. Matthäi, L. L. Mendes, N. Michailow, D. Zhang, and G. Fettweis, "Widely linear estimation for space-time-coded GFDM in low-latency applications," *IEEE Trans. Commun.*, vol. 63, no. 11, pp. 4501–4509, Nov. 2015.
- [15] D. Zhang, A. Festag, and G. Fettweis, "Performance of generalized frequency division multiplexing based physical layer in vehicular communication," *IEEE Trans. Veh. Technol.*, vol. PP, no. 99, pp. 1–1, 2017.
- [16] N. Michailow, I. Gaspar, S. Krone, M. Lentmaier, and G. Fettweis, "Generalized frequency division multiplexing: Analysis of an alternative multi-carrier technique for next generation cellular systems," in *Proc. 9th ISWCS*, Aug. 2012, pp. 171–175.
- [17] A. Farhang, N. Marchetti, and L. E. Doyle, "Low-complexity modem design for GFDM," *IEEE Trans. Signal Process.*, vol. 64, no. 6, pp. 1507–1518, March 2016.
- [18] P. Wei, X. G. Xia, Y. Xiao, and S. Li, "Fast DGT-based receivers for GFDM in broadband channels," *IEEE Trans. Commun.*, vol. 64, no. 10, pp. 4331–4345, Oct. 2016.

- [19] P. C. Chen, B. Su, and Y. Huang, "Matrix characterization for GFDM: Low complexity MMSE receivers and optimal filters," *IEEE Trans. Signal Process.*, vol. 65, no. 18, pp. 4940–4955, Sept. 2017.
- [20] A. Goldsmith, S. A. Jafar, I. Maric, and S. Srinivasa, "Breaking spectrum gridlock with cognitive radios: An information theoretic perspective," *Proc. IEEE*, vol. 97, no. 5, pp. 894–914, May 2009.
- [21] R. Datta, N. Michailow, S. Krone, M. Lentmaier, and G. Fettweis, "Generalized frequency division multiplexing in cognitive radio," in *2012 Proceedings of the 20th European Signal Processing Conference (EUSIPCO)*, Aug. 2012, pp. 2679–2683.
- [22] D. Panaitopol, R. Datta, and G. Fettweis, "Cyclostationary detection of cognitive radio systems using GFDM modulation," in *2012 IEEE Wireless Communications and Networking Conference (WCNC)*, April 2012, pp. 930–934.
- [23] G. Bansal, M. J. Hossain, and V. K. Bhargava, "Optimal and suboptimal power allocation schemes for OFDM-based cognitive radio systems," *IEEE Trans. Wireless Commun.*, vol. 7, no. 11, pp. 4710–4718, November 2008.
- [24] Y. Zhang and C. Leung, "Resource allocation in an OFDM-based cognitive radio system," *IEEE Trans. Commun.*, vol. 57, no. 7, pp. 1928–1931, July 2009.
- [25] S. Wang, F. Huang, and Z. H. Zhou, "Fast power allocation algorithm for cognitive radio networks," *IEEE Commun. Lett.*, vol. 15, no. 8, pp. 845–847, August 2011.
- [26] Ahmed A Rosas, Mona Shokair, and Sami A El_dolil, "Proposed optimization technique for maximization of throughput under using different multicarrier systems in cognitive radio networks," *EEEECEGC*, pp. 25–33, 2015.
- [27] A. E. Dawoud, A. A. Rosas, M. Shokair, M. Elkordy, and S. E. Halafawy, "PSO-adaptive power allocation for multiuser GFDM-based cognitive radio networks," in *2016 International Conference on Selected Topics in Mobile Wireless Networking (MoWNeT)*, April 2016, pp. 1–8.
- [28] D. W. K. Ng, E. S. Lo, and R. Schober, "Energy-efficient resource allocation in OFDMA systems with large numbers of base station antennas," *IEEE Trans. Wireless Commun.*, vol. 11, no. 9, pp. 3292–3304, Sept. 2012.